RERTR 2014 – 35TH INTERNATIONAL MEETING ON
REDUCED ENRICHMENT FOR RESEARCH AND TEST REACTORS

OCTOBER 12-16, 2014
IAEA VIENNA INTERNATIONAL CENTER
VIENNA, AUSTRIA

Residual Stress Measurement for Highly Radioactive Samples

M.B. Prime, M.L. Steinzig, D.E. Dombrowski, M.L. Lovato, D.J. Alexander,
K.D. Clarke, and F.Z. Broetto
W Division and MST Division
Los Alamos National Laboratory, PO Box 1663, Los Alamos, NM 87545 USA

ABSTRACT

The interface bonds are critical to in-reactor performance for a high density monolithic plate fuel system which uses low enriched uranium 10wt% molybdenum foils co-rolled with Zr and clad with 6061Al. Stresses induced during reactor shutdown have been identified as a source of concern for that integrity. Because of the post-reactor radioactivity, those residual stresses will have to be measured in a shielded nuclear radiation containment chamber or "hot cell" with remote handling of specimens and instrumentation, which limits measurement options. This study tested options for stress measurements by using surrogate fuel plates, such as with depleted uranium, but using only hot-cell appropriate equipment. Several measurements were performed using the incremental slitting method (a.k.a. crack compliance) but, for hot cell use, using a milling cutter instead of wire EDM for making the cut and a displacement sensor instead of a strain gauge. Measurements were also performed using incremental hole drilling using an interferometry system instead of strain gauges. For both measurement techniques, special data reduction development was required in order to handle discontinuities in the stress profiles across the layers. The results were encouraging, and the slitting method is now being implemented for use in a hot cell.

1. Introduction

The interface bonds are critical to in-reactor performance for a high density monolithic plate fuel system which uses low enriched uranium (LEU) 10wt% molybdenum foils co-rolled with Zr and clad with 6061Al. The RERTR-12 miniplate irradiation experiment resulted in a few of the higher-burnup plates exhibited pillowing, presumably a debonding of the Al cladding. The failure mode is not likely to occur in actual LEU fuel, because the LEU fuel is not only unable to reach the burnup attained in RERTR-12 plates, but also unable to sustain the power necessary for development of shutdown-induced stress at the end of irradiation [1]. Nonetheless, studying and understanding these failures aids the establishment of safe operating limits.

The current understanding of the pillowing of the fuel plates in RERTR-12 indicates that post-reactor-shutdown residual stresses are the most likely cause for the pillowing [1] and is summarized here. Finite element calculations with a creep model indicate that the fabrication stresses are relaxed by creep during operation, so fabrication stresses [2, 3] are not the concern. During operation, the LEU fuel is warm from the fission heating and the aluminum cladding is cooled by contact with the reactor coolant. The temperature in the fuel is uneven because of gradients in power and more efficient cooling of the fuel edges, and may be highest at an end of the plate. On shutdown, the entire fuel plate is rapidly cooled to the coolant temperature. The warm LEU fuel wants to contract as it cools but is constrained by the cladding and, therefore, ends up in tension. (Note that this is opposite to fabrication stresses where differential contraction from a uniform temperature puts the fuel into compression.) The post-shutdown stresses in the LEU fuel are highest where the fuel experienced the most radiation and, therefore, has the worst mechanical properties. The combination of high residual stress and degraded properties led to failure. There is an alternate failure hypothesis involving the pillowing being caused by fission gas pressure. The alternate hypothesis may be less likely because that would cause failure during operation rather than at shutdown, and no fission product leaks were detected in RERTR-12, but this hypothesis has not been convincingly disproven.

2. Scope – Need to Measure Specimens in Hot Cell

Predicting stresses under such multi-physics conditions is challenging and insufficiently predictive to be solely relied upon for important decisions. Therefore, to support root cause investigations and certification decisions, it is desired to instead measure residual stresses in fuel plates after reactor operation. Because of the very high radiological activity of fuel plates after reactor operation, such experiments would have to be performed in a shielded nuclear radiation containment chamber or “hot cell” with remote handling of specimens and instrumentation. Such hot cell testing will require changes to standard experimental procedures for residual stress measurement. This study examines the feasibility of using the incremental slitting method or incremental hole drilling within a hot cell. Experimental results are reported that test the most significant changes to standard procedure required for hot cell operation.

This paper summarizes work that is reported in much more detail in two reports, one for slitting [4] and one for hole drilling [5].

3. Technical Background

The method known most commonly as “crack compliance” but more descriptively called “incremental slitting” is a unique and valuable tool for residual stress measurement [6, 7]. By incrementally introducing a narrow slit and measuring relaxed strain at each increment of slit depth, $\varepsilon(a_i)$ see Figure 1, it is possible to precisely determine a depth profile of residual stresses, $\sigma_x(z)$. Slitting can be applied to a nearly limitless range of part thicknesses, with results having been reported for layer thicknesses as small as 300 nm [8] and part thicknesses greater 160 mm [9]. Slitting has measured stresses of very low magnitude quite precisely [10-13] and has been used on composites [14-18].

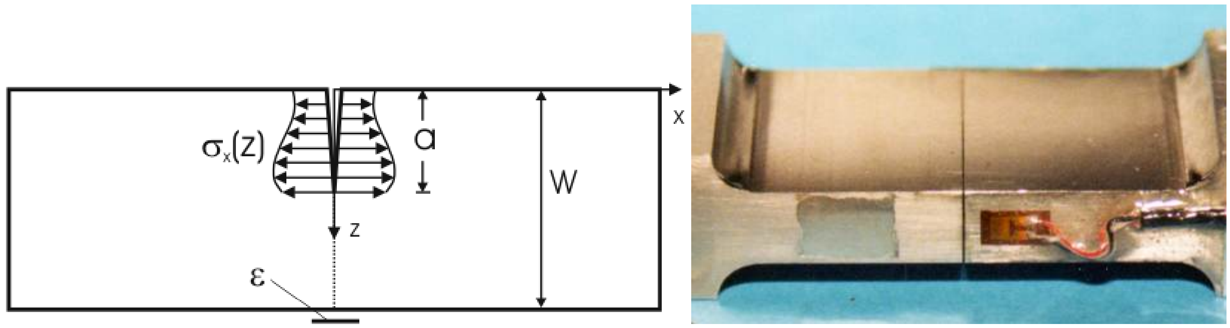

Figure 1. The incremental slitting method for measuring a depth profile (1-D) of residual stress.

The incremental hole drilling method [19] predates the slitting method, is standardized by ASTM [20], and is very widely used in industry. The principle is the same as for slitting but with a hole replacing a slit. Hole drilling is more commonly used for near-surface stress and slitting is more commonly used for through-thickness, but the capabilities overlap substantially.

3.1 Constraints for Hot Cell Operation and Changes to Experimental Procedure

The state-of-the-art for incremental slitting uses wire EDM to make the cut [7], because it can make a precise, narrow slit without introducing any machining stresses if the EDM is performed using skim cut settings [21]. A wire EDM is not currently available in the hot cell and is impractical because of its size and need for a large amount of dielectric fluid (deionized water) which would make for significant waste issues. For hot cell operation, conventional machining will need to be used to make the slit. As detailed in a literature review [22], prior to the advent of wire EDM, conventional machining in the form of a milling cutter or a circular saw on a mill was often used with the slitting method and excellent results could be obtained.

The state-of-the-art for incremental slitting and hole drilling both use standard electrical-resistance strain gauge(s) to measure the deformations [3, 19]. Unfortunately, the delicate operations required to bond a strain age and solder on lead wires are not feasible for remote operation in a hot cell. In this work, a displacement gauge is used to measure end-displacement of the specimen for slitting. Electronic Speckle Pattern Interferometry (ESPI) has been widely used with hole drilling [23-25] and offers the advantage of full-field data near the hole. ESPI was investigated here for use in the hot cell. The extra effort of implementing ESPI in a hot cell is potentially offset by the ability to obtain full-field information.

3.2 Theory

The incremental slitting method and incremental hole drilling use the same basic theory, and it is well described in several resources [7, 22]. The key assumption is that the stress relaxation and resulting deformations are all elastic. Solving the inverse problem to get stresses from the measured deformations is performed in this work using the pulse-regularization method [26], with modifications to allow for discontinuities in stress across the interfaces [3]. The hole drilling data was analyzed using the same inverse methodology but with an additional process to make best use of the full field ESPI data [24]. The calibration coefficients are calculated using a finite element model, which is standard practice [27, 28]. For slitting a 2D plane strain analysis gave the coefficients [29]. The calculation must model all *n* slit/hole depths, and for the *i*th slit/hole depth must calculate a coefficient for *i* pulse loads, making for $n \cdot (n-1)/2$ calculations. Abaqus software [30] was used along with the Python scripting interface, which allows for automation of the multiple calculations.

4. Experiments and results

4.1 Slitting Tests on Layered Surrogate Fuel Plates

Although not the main subject of this paper, results are presented from slitting measurements in 2012 on fuel plates using DU-10Mo as a surrogate for LEU-10Mo [3] to demonstrate the ability of the slitting method to resolve through-thickness stress profiles through the Aluminum and DU layers including discontinuities in stress across the interfaces. The results on DU-10Mo foils presented in the *next* section are more relevant for the experimental issues in a hot cell.

Figure 2a shows the stress profiles measured by slitting. Although the locations of the thin zirconium layers are indicated, they were too thin for their stresses to be independently identified by the measurements. The stress profiles show modest stress levels with significant discontinuities across the material interfaces. The stress magnitudes are limited by the flow strength of the 6061 Al. Testing revealed a 50 MPa yield strength and 140 MPa ultimate strength for Al 6061 put through the HIP cycle [31].

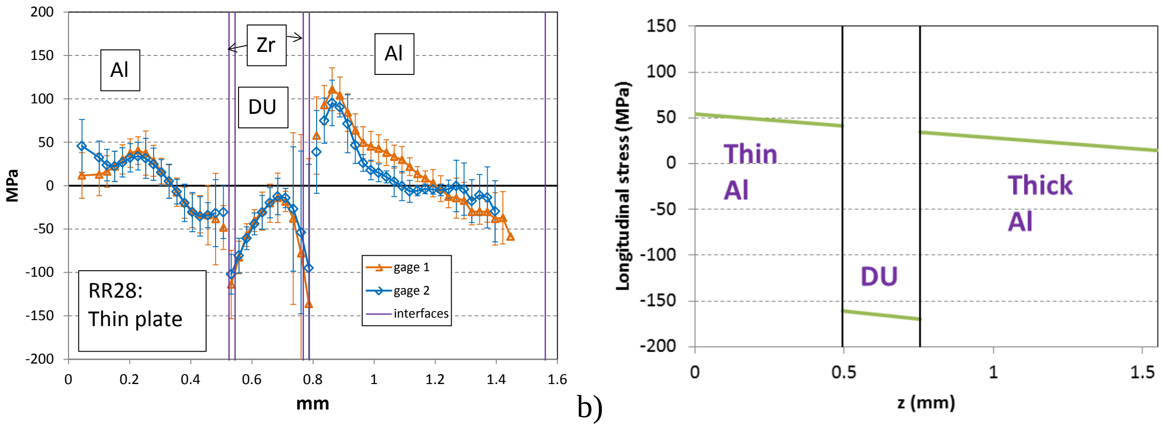

a) b)

Figure 2. a) Slitting test results for full surrogate fuel plates, from [3], and b) a simple thermal mismatch model that explains the basic features in the stress profile.

To aid interpreting the stresses, Figure 2b shows a model of the stress profile in the plate based on thermal expansion mismatch and elasticity. Because the model was meant to be explanatory rather than predictive, the temperature change was adjusted down to 200 ºC (compared to HIP ΔT of ~530 ºC) in order to get similar stress magnitudes to the measurements. The basic nature and slopes of the stress profiles in Figure 2a are well predicted by the thermal mismatch and the requirements of force and moment balance.

4.2 Slitting Tests Using Hot Cell Equipment on Foils

Foil coupons were prepared by bonding Zr to DU-10Mo foils and then a series of hot rolling passes, followed by annealing and then cold rolling to a final thickness of 0.58 mm including a

Zr thickness of about 0.021 mm on each face. A Keyence EX-110V inductive (eddy current) sensor[1] was used to measure cantilever end-displacement. To evaluate hot cell operations:

- One test was performed using wire EDM with both a strain gauge and the displacement sensor, see Figure 3a. Reducing the data independently for each instrument allowed the evaluation any loss of accuracy from using the displacement sensor.
- One test was performed using a mini mill with both a strain gauge and the displacement sensor, see Figure 3b. Reducing the data independently for each instrument allowed the evaluation any loss of accuracy from using a milling cutter instead of wire EDM, and then the combined effect of using both a milling cutter and a displacement sensor.

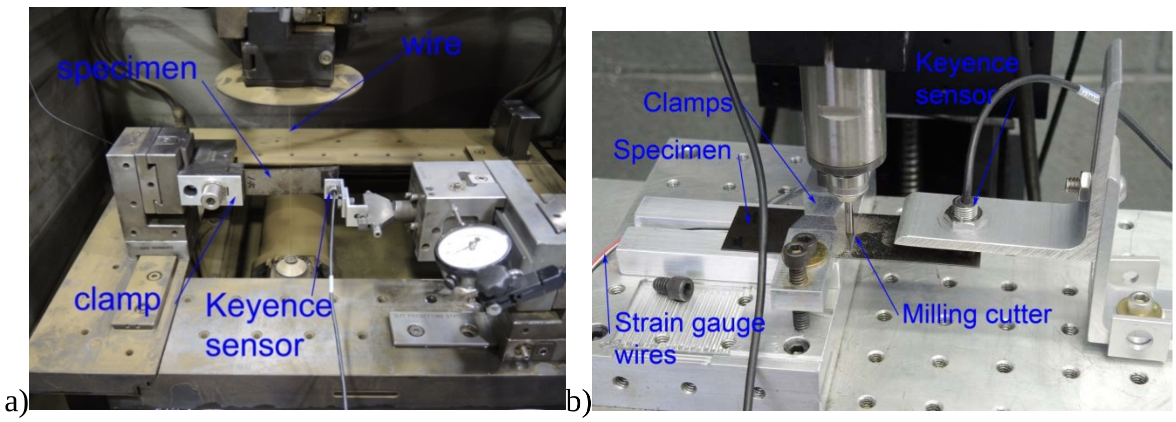

Figure 3. Slitting test setups for DU-10Mo foils using a) wire EDM and b) a mini-mill (right).

Figure 4 shows the data from both sets of tests, which look generally quite good. The mini-mill data looks somewhat different from the wire EDM data because the orientation of the specimen in the mini-mill (see Figure 3b) means that gravity loads add to those deformations. The gravity deformation were later subtracted from the data [4].

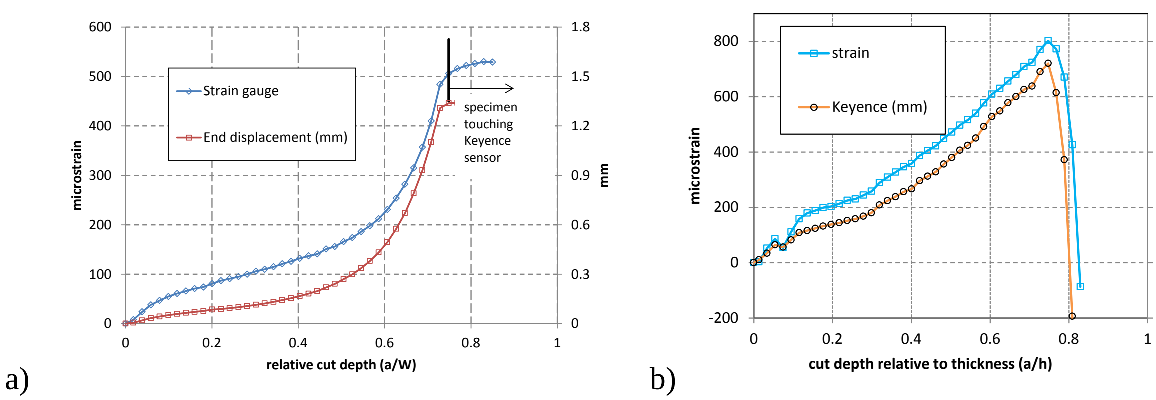

Figure 4. Slitting test data from a) wire EDM and b) a mini-mill.

Figure 5 shows the results for the slitting tests. Figure 5a shows the results for the wire EDM tests when the data was reduced separately using either the strain gauge data or the displacement data. The results agree within uncertainty until near the end of the test, when the specimen

[1] http://www.keyence.com/products/measure/inductive/ex-v/index.jsp

started to contact the displacement sensor. Figure 5b shows all four combinations of results: the mini-mill and wire EDM tests with strain or displacement data. Uncertainty bars are similar to the left figure but left off to keep the plot readable. Also plotted on the right figure are the stresses predicted by a simple thermal mismatch model for differential contraction of the Zr layer bonded to the DU-10Mo [4]. Although there was a small anomaly in the data from the mini-mill test [4], the results generally follow the expected trends of compressive stresses in the Zr layer balanced by modest tension in the DU-10Mo. Considering that the stresses in the DU are nearly zero, and the Zr stresses only occur over a depth of about 25 μm, the results is Figure 5 are quite good. The post-shutdown stresses in LEU fuel plates are expected to be much more significant.

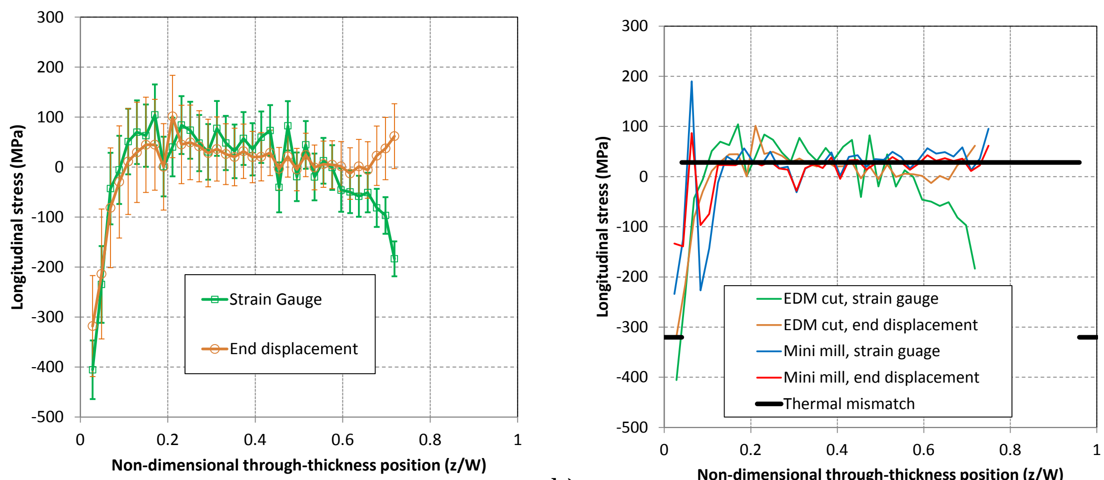

a) b)

Figure 5. Slitting test results showing a) that results are the same using a strain gauge or displacement gauge and b) that all of the results give the general stress distribution expected from thermal mismatch.

4.1 Hole drilling Tests on Layered Surrogate Fuel Plates

Because of the safety-related difficulties of measuring residual stress in materials containing uranium, surrogate plates with dimensions similar to those of the actual RERTR fuel plates were fabricated at Los Alamos National Laboratory. These surrogate fuel plates substituted 304 stainless steel foils for the uranium foils, and HIP'd the foils to 6061 aluminum plates. Figure 6 shows the hole drilling setup using ESPI and Figure 7 shows typical data.

Figure 8 shows typical results from measurements made in the surrogate plates, which were analyzed using different algorithms for the portion of the data analysis handling the full-field data. Qualitatively, the results from both algorithms show a low state of stress in the top section of aluminum that is initially drilled, followed by a transition to a different state of stress in the stainless steel, and then a second transition in the back section of aluminum. Quantitatively, the two algorithms produce significantly different results, which is probably the result of errors in the implementation of the new set of coefficients generated for the thin plate analysis. Additional work would be required to correct this anomaly. The stress levels in the second Al layer are too high to be possible for Al 6061 put through the HIP cycle [31].

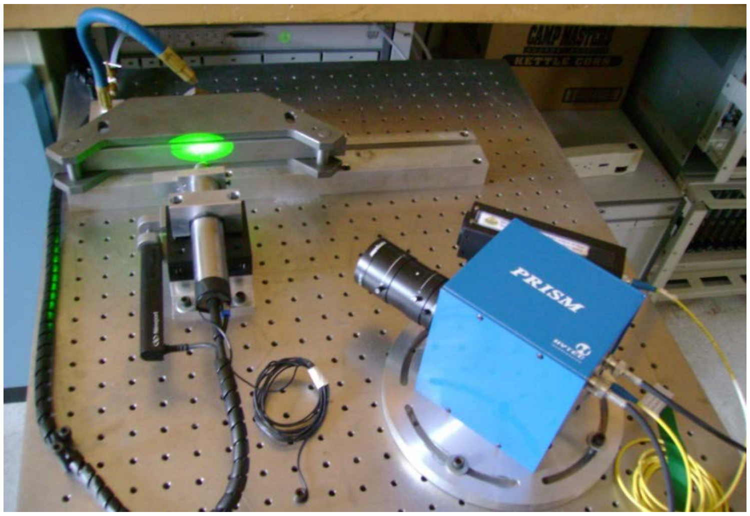

Figure 6. Setup for hole drilling tests showing calibration sample.

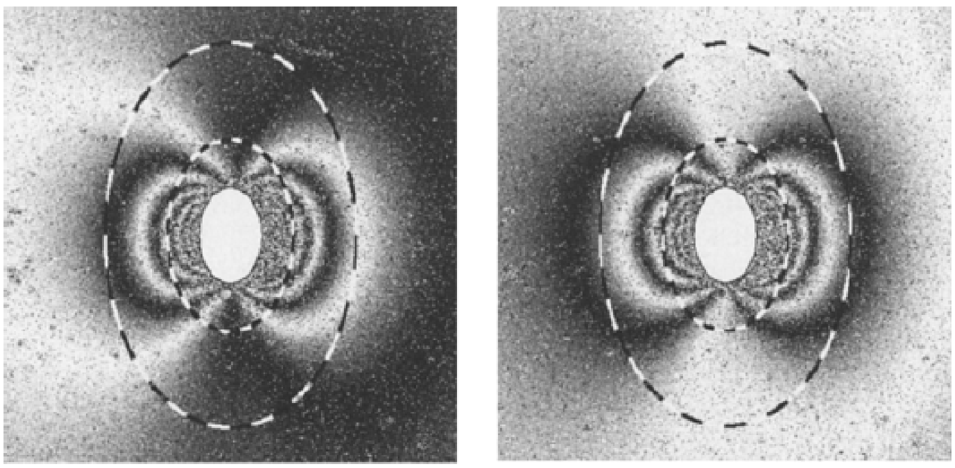

Figure 7. Measured fringe pattern from a drilled hole (left) and same data after rigid body motion has been removed.

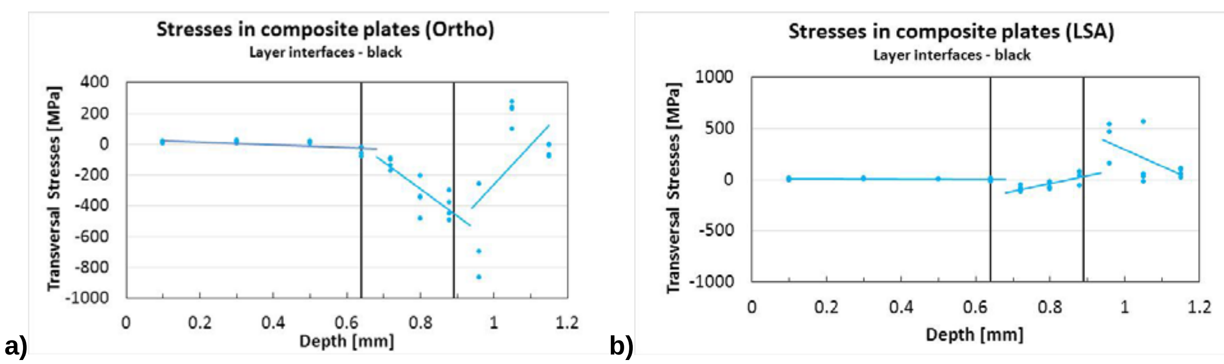

Figure 8. Transverse stresses measured in surrogate plate and analyzed using a) the orthogonal algorithm and b) the Least Squares algorithm.

4. Discussion and Conclusions

Both incremental slitting and hole drilling were being considered to measure residual stress in the hot cell. Incremental slitting provides different information from that which could be provided by hole drilling with different risk. Figure 9 defines a coordinate system for the fuel plate for use with Table 1, which compares the two methods for use in a hot cell. In general, hole drilling has more flexibility to provide a spatial map of stresses, with the exception that the slitting method is more suited to resolving a depth profile all the way through the part thickness. Overall, the mapping provided by hole drilling would be more detailed in regions of possible concern, such as near the edges of the LEU fuel. The hole drilling measurements would be more expensive and more risky. The laser-based deformation measurements require laser and optical access, a camera for recording the results, and some level of vibration isolation.

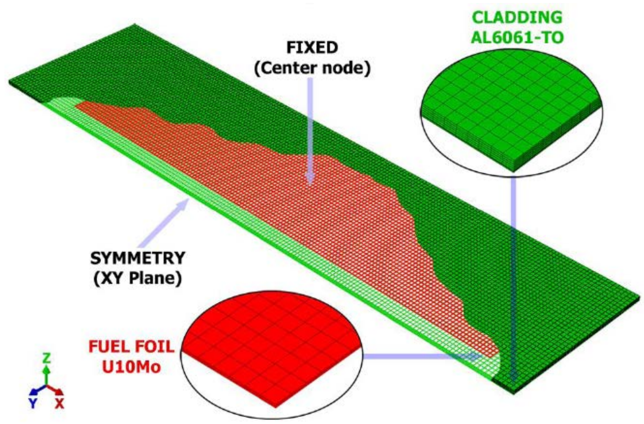

Figure 9. Coordinate definition for fuel plate: x is longitudinal direction, y is transverse, and z through-thickness. Figure taken from presentation by Hakan Ozaltun, INL.

	Slitting	Hole Drilling
Spatial Mapping	$\sigma_x(z)$ at different x locations	$\sigma_x(z)$, $\sigma_y(z)$, $\tau_{xy}(z)$ at different (x,y) locations
Through thickness	Good resolution through most of specimen thickness	Ability to resolve stresses degrades ≈ halfway through plate thickness
Machining	A small mill with two translation axes (plunge depth and lateral translation)	A small mill (dental drill is often used) with one translation axis (depth)
Deformation measurement	Displacement transducer	Electronic Speckle Pattern Interferometry (ESPI), laser-based.
Calibration coefficients	A 2-D elastic, finite element model provides coefficients for data reduction. Easily scripted.	A 3-D elastic, finite element model is required and must be customized for different hole locations.
Cost and risk	Modest	More significant because of laser-based ESPI technique.

Table 1. Comparison of methods

The slitting results are currently more believable than the hole drilling results based on the agreement with simple thermal expansion mismatch calculations and comparisons with neutron data [2]. It is expected that hole drilling could provide as good results with more work to improve the data analysis. However, the selection was made to proceed with the slitting method as the primary option for hot cell measurements. ESPI hole drilling is still being pursued as a second option for future measurements.

5. Acknowledgements

Los Alamos National Laboratory, an affirmative action/equal opportunity employer, is operated by the Los Alamos National Security, LLC for the National Nuclear Security Administration of the U.S. Department of Energy under contract DE-AC52-06NA25396.

6. References

[1] Medvedev, P. G., Ozaltun, H., Robinson, A. B., and Rabin, B. H., 2014, "Shutdown-induced tensile stress in monolithic miniplates as a possible cause of plate pillowing at very high burnup," Proc. The European Research Reactor Conference, RRFM 2014, Ljubljana, Slovenia, European Nuclear Society, pp. 134-141.

[2] Brown, D. W., Okuniewski, M. A., Almer, J. D., Balogh, L., Clausen, B., Okasinski, J. S., and Rabin, B. H., 2013, "High energy X-ray diffraction measurement of residual stresses in a monolithic aluminum clad uranium–10wt% molybdenum fuel plate assembly," Journal of Nuclear Materials, 441(1–3), pp. 252-261.

[3] Prime, M. B., and Crane, D. L., 2014, "Slitting Method Measurement of Residual Stress Profiles, Including Stress Discontinuities, in Layered Specimens," Residual Stress, Thermomechanics & Infrared Imaging, Hybrid Techniques and Inverse Problems, Volume 8, Conference Proceedings of the Society for Experimental Mechanics Series, M. Rossi, M. Sasso, N. Connesson, R. Singh, A. DeWald, D. Backman, and P. Gloeckner, eds., Springer International Publishing, pp. 93-102.

[4] Prime, M. B., Lovato, M. L., Alexander, D. J., Beard, T. V., Clarke, K. D., and Folks, B. S., 2014, "Incremental Slitting Residual Stress Measurements for a Hot Cell," LA-UR-14-23273, Los Alamos National Laboratory.

[5] Steinzig, M., and Broetto, F. Z., 2014, "Residual Stress measurements in thin composite plates using the hole drilling technique," LA-UR-14-23956, Los Alamos National Laboratory.

[6] Cheng, W., and Finnie, I., 2007, Residual Stress Measurement and the Slitting Method, Springer Science+Business Media, LLC, New York, NY, USA.

[7] Hill, M. R., 2013, "The Slitting Method," Practical Residual Stress Measurement Methods, G. S. Schajer, ed., John Wiley & Sons, Ltd, pp. 89-108.

[8] Sabate, N., Vogel, D., Gollhardt, A., Keller, J., Cane, C., Gracia, I., Morante, J. R., and Michel, B., 2006, "Measurement of residual stress by slot milling with focused ion-beam equipment," Journal of Micromechanics and Microengineering, 16(2), pp. 254-259.

[9] Cheng, W., and Finnie, I., 1993, "Measurement of residual stress distributions near the toe of an attachment welded on a plate using the crack compliance method," Engineering Fracture Mechanics, 46(1), pp. 79-91.

[10] Prime, M. B., and Hill, M. R., 2002, "Residual stress, stress relief, and inhomogeneity in aluminum plate," Scripta Materialia, 46(1), pp. 77-82.

[11] Aydiner, C. C., Ustundag, E., Prime, M. B., and Peker, A., 2003, "Modeling and measurement of residual stresses in a bulk metallic glass plate," Journal of Non-Crystalline Solids, 316(1), pp. 82-95.

[12] Dalle Donna, C., Lima, E., Wegner, J., Pyzalla, A., and Buslaps, T., 2001, "Investigations on Residual Stresses in Friction Stir Welds," Proc. 3nd International Symposium on Friction Stir Welding, 27 and 28 September 2001, Kobe, Japan, The Welding Institute TWI, UK, p. pdf/CDrom.

[13] Wang, Q. C., Hu, X. D., Li, W., and Yuan, J. L., 2006, "Numerical simulation of machining distortion of residually stressed aircraft aluminum components," Key Engineering Materials, 315/316, pp. 235-238.

[14] Gungor, S., 2002, "Residual stress measurements in fibre reinforced titanium alloy composites," Acta Materialia, 50(8), pp. 2053-2073.
[15] Shokrieh, M. M., and Akbari R, S., 2012, "Effect of Residual Shear Stresses on Released Strains in Isotropic and Orthotropic Materials Measured by the Slitting Method," Journal of Engineering Materials and Technology, 134(1), pp. 011006-011009.
[16] Akbari, S., Taheri-Behrooz, F., and Shokrieh, M. M., 2013, "Slitting Measurement of Residual Hoop Stresses Through the Wall-Thickness of a Filament Wound Composite Ring," Experimental Mechanics, 53(9), pp. 1509-1518.
[17] Shokrieh, M., Daneshvar, A., Akbari, S., and Chitsazzadeh, M., 2013, "The use of carbon nanofibers for thermal residual stress reduction in carbon fiber/epoxy laminated composites," Carbon, 59, pp. 255-263.
[18] Hill, M. R., and Lin, W. Y., 2002, "Residual stress measurement in a ceramic-metallic graded material," Journal of Engineering Materials and Technology, 124(2), pp. 185-191.
[19] Schajer, G. S., and Whitehead, P. S., 2013, "Hole Drilling and Ring Coring," Practical Residual Stress Measurement Methods, G. S. Schajer, ed., John Wiley & Sons, Ltd, pp. 29-64.
[20] 2008, "ASTM standard E 837–08," Standard Test Method for Determining Residual Stresses by the Hole-Drilling Strain-Gage Method, ASTM International.
[21] Cheng, W., Finnie, I., Gremaud, M., and Prime, M. B., 1994, "Measurement of near-surface residual-stresses using electric-discharge wire machining," Journal of Engineering Materials and Technology, 116(1), pp. 1-7.
[22] Prime, M. B., 1999, "Residual stress measurement by successive extension of a slot: The crack compliance method " Applied Mechanics Reviews, 52(2), pp. 75-96.
[23] Steinzig, M., and Ponslet, E., 2003, "Residual Stress Measurement Using The Hole Drilling Method And Laser Speckle Interferometry: Part I," Experimental Techniques, 27(3), pp. 43-46.
[24] Schajer, G. S., and Steinzig, M., 2005, "Full-field calculation of hole drilling residual stresses from electronic speckle pattern interferometry data," Experimental Mechanics, 45(6), pp. 526-532.
[25] Nelson, D. V., and McCrickerd, J. T., 1986, "Residual-stress determination through combined use of holographic interferometry and blind-hole drilling," Experimental Mechanics, 26(4), pp. 371-378.
[26] Schajer, G. S., and Prime, M. B., 2006, "Use of Inverse Solutions for Residual Stress Measurements," Journal of Engineering Materials and Technology, 128, pp. 375-382.
[27] Lee, M. J., and Hill, M. R., 2007, "Effect of strain gage length when determining residual stress by slitting," Journal of Engineering Materials and Technology, 129(1), pp. 143-150.
[28] Rankin, J. E., Hill, M. R., and Hackel, L. A., 2003, "The effects of process variations on residual stress in laser peened 7049 T73 aluminum alloy," Materials Science & Engineering A, A349(1/2), pp. 279-291.
[29] Aydiner, C. C., and Prime, M. B., 2013, "Three-Dimensional Constraint Effects on the Slitting Method for Measuring Residual Stress," Journal of Engineering Materials and Technology, 135, pp. 031006-031001.
[30] Simulia Abaqus 5.12-1 Dassualt Systems, 2012.
[31] Alexander, D. J., Clarke, K. D., Liu, C., and Lovato, M. L., 2011, "Tensile Properties of 6061 Aluminum Alloy Materials," Los Alamos National LAboratory report LA-UR-11-06707.